A TWO-DIMENSIONAL INTAKE MANIFOLD FLOW SIMULATION

Peter Li

Scientific Research Laboratory, Ford Motor Company
20000 Rotunda, Dearborn, Michigan 48121

ABSTRACT. A computer flow model of an intake manifold of a four cylinder engine has been developed using a computational fluid dynamic code. This code is based on the Conchas-Spray code developed at the Los Alamos National Laboratory. The flow inside the intake manifold is assumed to be two-dimensional, unsteady, compressible, and turbulent. A simple subgrid scale (SGS) turbulence model and hypothetical boundary conditions are employed in the simulation. Atmospheric pressure is specified at the inlet and the velocities are specified at the outlets of the manifold, together with the law of the wall at all the wall boundaries. Numerical results of the simulation are presented in the form of velocity, pressure, density, and temperature fields. The model is designed in such a way that different manifold geometries may be simulated with ease. A simulation of a concept manifold "the loop-manifold" is also presented.

Keywords. Computational Fluid Dynamics; Intake Manifold; Flow simulation; Engine induction; Turbulence flow.

INTRODUCTION

The Performance of an internal combustion engine, be it power, fuel economy or emissions, is strongly influenced by the combustion of the air and fuel inside an engine cylinder. This combustion process is strongly affected by the in-cylinder 'support flow' that results from the transport of the air and fuel through the induction system. The understanding of the effect of the induction geometry on the support flow is therefore essential for internal combustion engine development.

The task of describing and understanding the fluid flows inside the complex induction geometries is difficult. This is due to the multi-dimensionality of the flow geometry, and the highly transient operation of the automotive engine. There are many research studies, experimental and theoretical, trying to understand this difficult problem. Most theoretical work includes mostly zero-dimensional (Sullivan, 1978; Wu, 1983) or one-dimensional (Benson, 1971; Low, 1981; Chapman, 1982) approaches. Only recently have there been reported two-dimensional studies on this problem (Chapman, 1979). This study presents a two-dimensional model of the flow inside an intake manifold. The flow is assumed to be unsteady, compressible nd turbulent. A set of partial differential equations that describe this flow problem includes the continuity equation, two momentum equations and the simple SGS turbulence model (Deardorff, 1971). These equations are coupled, non-linear, unsteady with very complex geometry. To solve such internal recirculating turbulent flow problems is very difficult. Pure analytical treatment of such problems is of course generally impossible. However, advancements in computer technology, numerical techniques, and flow measurement techniques in the last few decades, together with the immense need in industry prompted many concentrated research activities in this area. This is reflected by the large number of recent publications and conferences devoted to this type of problem. These have of course resulted in the formulation of several models, which allow the mathematical description of such turbulent flows with a close set of elliptic partial differential equations. These lead to the development of a number of computational codes with which multi- dimensional flow simulation is possible (Hirt, 1971; Amsden, 1973; Pracht, 1976; Gosman, 1977; Cloutman, 1982).

Among these codes, an in-house modified version of the CONCHAS-SPRAY code (Cloutman, 1982) from Los Alamos National Laboratories is used in this study. The purpose of this report is to discuss our extended development of this code as applied to induction flow research, and a particular application to the simulation of air flow inside a 1.6 liter intake manifold.

INTAKE MANIFOLD FLOW MODEL

The Flow Geometry

The manifold (Figure 1) is idealized to be two-dimensional (Figure 2). The flow in the manifold is unsteady, compressible and turbulent. The governing equations together with the boundary and initial conditions that form the mathematical problem are given below. The computational code is then used to numerically solve this problem.

Governing Equations

Direct solution of the Navier-Stokes equations to resolve all scale of turbulence is yet to be realized. Thus, approximate "mean" equations have to be used to describe the flow. There are various ways of averaging that have been reported in the literature (Schlichting, 1968; Deardorff, 1971; Launder, 1972). The resulting "mean" governing equations for the two dimensional turbulent, compressible, unsteady flow in the Cartesian coordinates are given below:

Continuity equation,

$$\frac{\partial \rho}{\partial t} + \frac{\partial (\rho U)}{\partial X} + \frac{\partial (\rho V)}{\partial Y} = 0 \qquad (1)$$

Momentum equations,

$$\rho\left(\frac{\partial U}{\partial t}+U\frac{\partial U}{\partial X}+V\frac{\partial U}{\partial Y}\right)=-\frac{\partial P}{\partial X}+GX+\mu\left[\frac{\partial^2 U}{\partial X^2}+\frac{\partial^2 U}{\partial Y^2}\right]+\frac{1}{3}\mu\frac{\partial}{\partial X}\left[\frac{\partial U}{\partial X}+\frac{\partial V}{\partial Y}\right] \quad (2)$$

$$\rho\left(\frac{\partial V}{\partial t}+U\frac{\partial V}{\partial X}+V\frac{\partial V}{\partial Y}\right)=-\frac{\partial P}{\partial Y}+GY+\mu\left[\frac{\partial^2 V}{\partial X^2}+\frac{\partial^2 V}{\partial Y^2}\right]+\frac{1}{3}\mu\frac{\partial}{\partial Y}\left[\frac{\partial U}{\partial X}+\frac{\partial V}{\partial Y}\right] \quad (3)$$

The internal energy equation,

$$\rho\left(\frac{\partial e}{\partial t}+U\frac{\partial e}{\partial X}+V\frac{\partial e}{\partial Y}\right)=-P\left(\frac{\partial U}{\partial X}+\frac{\partial V}{\partial Y}\right)+\frac{\partial}{\partial X}\left(k\frac{\partial T}{\partial X}\right)+\frac{\partial}{\partial Y}\left(k\frac{\partial T}{\partial Y}\right)+\phi+\frac{\partial q}{\partial t} \quad (5)$$

where

$$\phi=\mu\left[2\left\{\left(\frac{\partial U}{\partial X}\right)^2+\left(\frac{\partial V}{\partial Y}\right)^2\right\}+\left(\frac{\partial U}{\partial Y}+\frac{\partial V}{\partial X}\right)^2-\frac{2}{3}\left(\frac{\partial U}{\partial X}+\frac{\partial V}{\partial Y}\right)^2\right]$$

Ideal gas is assumed and

$$P=\rho R_g T \quad (6)$$

where X - horizontal coordinate
Y - vertical coordinate
U - velocity component in X direction
V - velocity component in Y direction
ρ - fluid density
t - time
μ - "mean"viscosity
P - pressure
GX,GY - body forces
e - specific internal energy
q - internal heat generation
T - temperature
k - "mean" thermal conductivity
ϕ - viscous dissipation function
R_g - universal gas constant

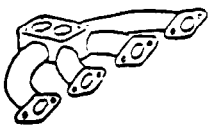

Figure 1. The 1.6l intake manifold.

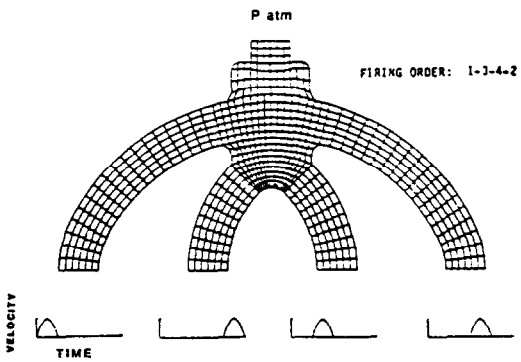

Figure 2. Numerical mesh genrated by the pre-processor and the boundary conditions used.

The "mean" equations given above retain the form of the Navier-Stokes equations. The difference only lies in the expression of the transport coefficients (i.e. viscosity, thermal conductivity). For the exact Navier-Stokes equations, these coefficients are properties of the fluid only, while for the "mean" equations, these coefficients also depend on the "mean" flow field. There are many turbulence models that define the relationships of these coefficients to the "mean" flow field. These models come in varying levels of complexity, i.e. mixing length model (Schlichting, 1968), 1-equation model, k-ϵ model (Launder, 1972), SGS model (Deardorff, 1971), etc..

The subgrid scale (SGS) model suggested by Deardorff (1971) is used in this study. This SGS model accounts for turbulence whose scale is smaller than the computational grid size, and resolves the larger scale turbulence numerically. A simplified version of the model for two-dimensional problems is given as,

$$\mu_t=\frac{1}{2}k_d^2\lambda^2\left(D_{11}^2+D_{22}^2+2D_{12}^2\right) \quad (7)$$

where

$$D_{11}=2\frac{\partial U}{\partial X},\quad D_{22}=2\frac{\partial V}{\partial Y},\quad D_{12}=\frac{\partial U}{\partial Y}+\frac{\partial V}{\partial X},$$

k_d = 0.17, an empirical constant,
λ = 0.3, average cell size.

Note that physically, turbulence flow is three-dimensional. An inherent consequence of the two-dimensional flow assumption with this simple turbulence model is that only the smaller scale (cell size) three-dimensional turbulence is accounted for by the model, while larger scale turbulence is assumed two-dimensional and resolved numerically.

The Boundary Conditions

Figure 2. shows the discretized flow geometry and the corresponding boundary conditions used in the simulation. At the runner outlets, the induction process is simulated by specifying a hypothetical outlet flow velocity. For convenience, the flow velocity is assumed to be spatially uniformed and a half sinusoid in time. The engine firing order is 1-3-4-2. The outlet boundary conditions for one complete engine cycle or two engine revolutions are given as

$$V_{r\#1}=\begin{cases}V_{max}*\sin(CA) & 0^\circ<CA<180^\circ\\ 0 & \text{elsewhere}\end{cases} \quad (8)$$

$$V_{r\#2}=\begin{cases}V_{max}*\sin(CA) & 540^\circ<CA<720^\circ\\ 0 & \text{elsewhere}\end{cases}$$

$$V_{r\#3}=\begin{cases}V_{max}*\sin(CA) & 180^\circ<CA<360^\circ\\ 0 & \text{elsewhere}\end{cases}$$

$$V_{r\#4}=\begin{cases}V_{max}*\sin(CA) & 360^\circ<CA<540^\circ\\ 0 & \text{elsewhere.}\end{cases}$$

Where V_r = air velocity at runner outlet.
V_{max} = maximum outlet velocity.
CA = t*6*RPM - crank angle.
t = time in seconds.
RPM = engine speed.

At the manifold inlet, wide open throttle is simulated by letting the inlet pressure be atmospheric, neglecting the effects of air ducts upstream of the air cleaner, or

$$P_{inlet}=P_{atm}. \quad (9)$$

The law of the wall is used on the solid boundaries (Schlichting, 1968). For a turbulent boundary layer this is

$$\frac{U}{U_*} = 2.5 \ln \left(\frac{y_w U_*}{\nu}\right) + B. \quad (10)$$

Where U = the tangential velocity at Y_w,
Y_w = distance from the wall,
ν = the kinematic viscosity,
B = the wall roughness constant (B=5.5 smooth wall),
U_* = the wall shear speed.

The wall shear speed is defined in term of the wall shear stress τ_w as

$$\tau_w = \rho U_*^2. \quad (11)$$

Replacing the U_* on the right hand side of the equation (10) with the 1/7-law (Schlichting, 1968) approximation U_*^S, which is

$$\frac{y_w U_*^S}{\nu} = 0.15 \left(\frac{y_w U}{\nu}\right)^{7/8} \quad (12)$$

eliminates the transcendental nature of the equation with respect to U_*. For smooth wall (B=5.5) equation (8) becomes,

$$\frac{U}{U_*} = .75 + 2.19 \ln \left(\frac{y_w U}{\nu}\right). \quad (13)$$

Equation (13) is used for $y_w U/\nu > 130.3$. However, for $y_w U/\nu < 130.3$, equation (13) is replaced by the laminar sublayer formula

$$\frac{U}{U_*} = \left(\frac{y_w U}{\nu}\right)^{1/2}. \quad (14)$$

For simplicity, the thermal boundary layer is approximated using the Reynolds analogy. Thus for turbulent flow, the heat flux is given as

$$q = 1.125 \left(\frac{\tau}{U}\right) c_p (T - T_w). \quad (15)$$

Where
q = heat flux to wall
c_p = specific heat at constant pressure
T_w = wall temperature
T = fluid temperature.

This is the same formula used by Cloutman (1982). Again for the laminar sublayer, equation (15) is replaced by

$$q = 1.125 \rho \nu c_p \left(\frac{T - T_w}{y}\right). \quad (16)$$

which is a simple difference approximation to the laminar heat flux with Prandtl number equaling 0.89. For simplicity, t_w is assumed to be constant along the wall boundary and equal to 343°K.

The Initial Conditions

The air inside the manifold is assumed to be quiescent in the beginning. The initial pressure is assumed atmospheric. The initial temperature is assumed to be 343 degrees kelvin.

The Computer Code

A computer code called Flody is used to numerically solve the flow simulation problem given above. It is a modified version of the Conchas-Spray code (Cloutman, 1982). Extensive modification is made to include inflow and outflow boundary conditions. For this study, combustion and spray are excluded. A preprocessor and a postprocessor allowing easy specification of the flow problem and expedient output presentation are added. A brief description of the numerical scheme is given here.

Flody is a time marching procedure that solves the finite difference approximation of the governing equations given above. The transient solution is semi-implicit. It uses spatial differences in the generalized quadrilateral cells. The corners of the cells, called vertices, are allowed to arbitrarily move in time. These allow a Lagrangian and/or Eulerian description. This type of mesh, known as the arbitrary Lagrangian-Eulerian (ALE) mesh (Hirt, 1971; Amsden,1973; Pracht, 1976), is particularly useful in representing curved and/or moving boundary surfaces. The spatial differencing is made conservative wherever possible. The procedure used differences the basic equations in the integral form. The divergence terms are transformed into surface (line) integrals over the local cell boundary. The approach is known as the ICED method (Stein, 1977; Tunstall, 1977). This ICED-ALE method is also found in other codes such as the YAQUI (Amsden, 1973), BAAL (Pracht, 1976), YOKIFER (Anderson, 1975), SALE (Amsden, 1980), and CONCHAS (Butler, 1979). For more detailed information on the numerical scheme see reference (Cloutman, 1982).

RESULTS AND DISCUSSIONS

The flow inside the idealized intake manifold is calculated for a duration of two complete engine cycles (or four engine revolutions). The Flody code on the Dec 20 computer is used. Total cpu time for the simulation is approximately 50 hours. The computational grid and boundary conditions used are shown in Figure 2. Some numerical results are presented below. Figure 3 is a sequence of pictures that show the development of the flow field during the induction of runner #1. The plots presented are for the second engine cycle. The flow fields are represented by velocity vectors showing their direction and magnitude. The plots exhibit the complex nature of the highly transient induction process. For example, note how two large residual vortices in the manifold plenum affect the development of the subsequent flow field. This is apparent during the beginning of the induction where the flow is routed around the two vortices. However, when the flow increases to its peak value it becomes less dependent on the flow history, and more dependent on the upstream and boundary conditions. This can be observed from the presence of a main column of air with large velocity that flows through the main runner. Note how the two vortices generated on the sides of this column grow during the later part of the induction and move into the plenum, thus affecting the induction through the next runner. The unsteady flow inside the manifold is complicated because of the interactions of both the manifold flow history (initial condition) and the complex manifold geometry (boundary condition), and the compressibility effect. Observe for example, the flow near the outlet of runner #1. If the flow were steady, one would expect the bending of the runner to cause the velocity distribution to be skewed outward (maximum velocity shifted toward the outside wall of the manifold). The simulation results however show otherwise. Such effects demonstrate the need for numerical simulation of such complex flows.

Figure 4 shows in a sequence of three pictures the variation of the pressure field during the induction of runner #1. The first picture corresponds to the beginning of the induction when the flow is accelerating. The second picture corresponds

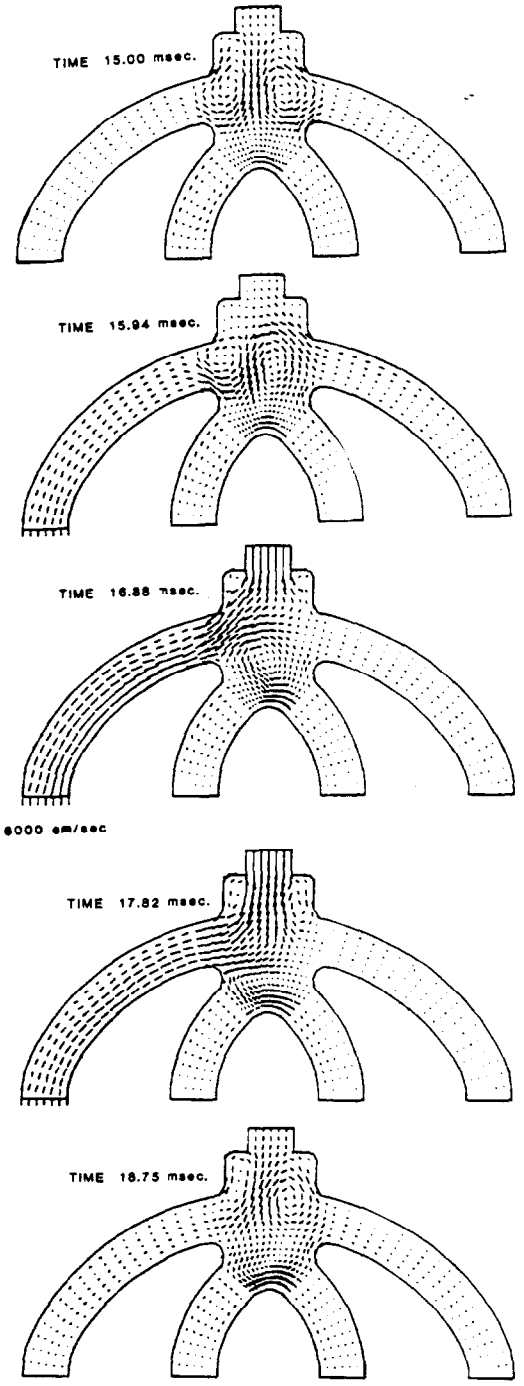

Figure 3. Flow development during induction of runner #1.

to the midpart of the induction when the flow is maximum, and the last picture corresponds to the later part of the induction when the flow is decelerating. During acceleration and deceleration the pressure appears constant throughout the cross section of the runner, varying only along the flow direction. These show the dominance of the acceleration forces during these periods. The pressure decreases along the runner during acceleration and increases during deceleration. This

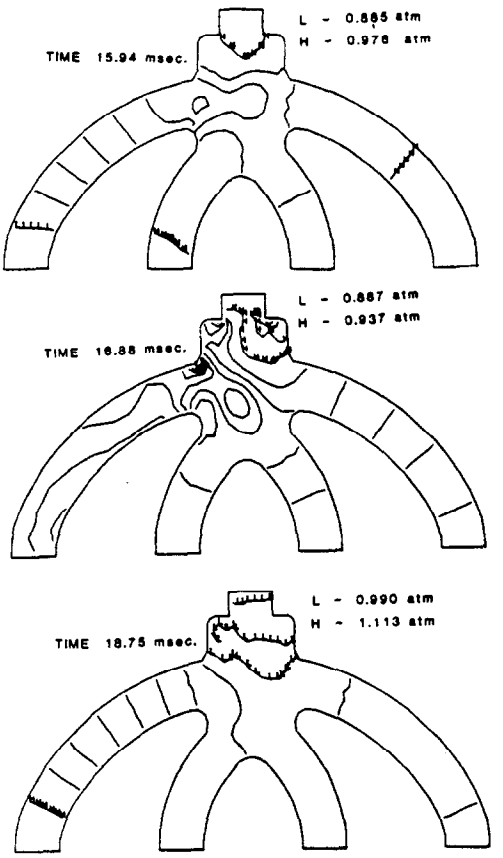

Figure 4. Development of pressure field during induction of runner #1.

shows that perhaps one-dimensional flow simulation during these two periods may be adequate. On the other hand, the second picture in figure 4 shows that during peak flow, when the flow is neither accelerating nor decelerating, the pressure field is two-dimensional. Larger concentration of pressure lines is observed near corners and cross section changes, indicating where a large portion of the manifold losses occur. Figures 5 and 6 plot the density and the temperature distributions during maximum induction flow in runner #1. Notice that they are rather complicated.

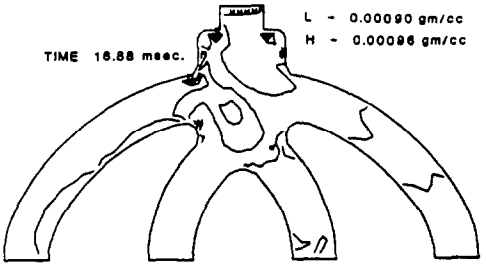

Figure 5. Constant density line during peak flow in runner #1.

Figure 7 shows the temporal variation of the pressure at each of the four runner outlets. The first 15 milliseconds correspond to the induction of

runner #1. The line plot clearly shows the pressure dip during acceleration of the flow, the crossover during peakflow, and the surge during flow deceleration. This definitely is different from the quasi- steady assumption, where temporal variation of the pressure would have been symmetrical during acceleration and deceleration. Subsequent fluctuations of the pressure in runner #1

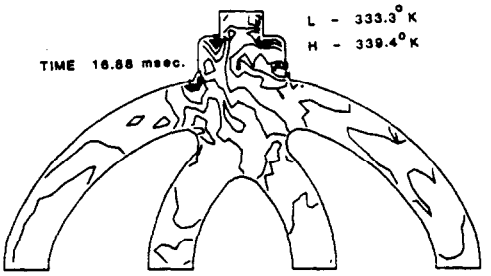

Figure 6. Isotherm in manifold during peak flow in runner #1.

during the induction of other runners are due to the air compressibility. Comparison of the pressure fluctuations of all four runners shows the pressure fluctuations of runners #1 and #4 are quite similar when shifted temporally. The same is true with runners #2 and #3. But, the fluctuations of #1 and #4 are both larger than those of #2 and #3. This is associated with the difference in the runners' length. This demonstrates the capability of the two-dimensional fluid code in simulating such complicated manifold dynamics.

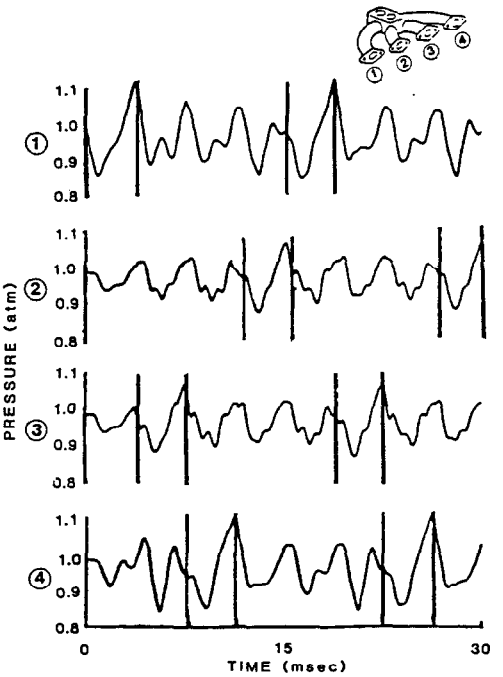

Figure 7. Pressure dynamics at outlets of 1.61 manifold.

The manifold efficiency (η) is used to measure the performance of the intake manifold. In this study, η is calculated for each of the four runners and is defined as

$$\eta_{\#n} = \frac{M_{a\#n}}{M_{itot}} X100\% \qquad (17)$$

where η = volumetric efficiency,
#n = runner's number (1,2,3,4)
M_a = actual mass flow rate,
M_{itot} =total ideal mass flow rate.

M_a is the time integral of the volume flow rate multiplied by the fluid density at the runner's outlet, while M_{itot} is time integral of the volume flow rate multiplied by the manifold inlet density (i.e., atmospheric). The efficiency for the 1.6 liter manifold is calculated based on the numerical data for the two engine cycles simulated. The results are tabulated in table 1 below.

Table 1. Manifold Efficiency η (%)

runner	#1	#2	#3	#4	TOTAL
1.61-manifold	23.6	23.7	23.8	23.7	94.8
loop-manifold	24.2	24.0	24.1	24.2	96.4

The Loop Manifold

An attractive feature of "Flody" is the ease with which the geometry can be changed. As an example, the flow inside a concept loop-manifold (Figure 8) is simulated by simply changing the geometry outline in the code. The initial and boundary conditions used are those of the 1.61 intake manifold. Results are summarized by the temporal pressure variations in Figure 9 and the manifold efficiency tabulated in table 1. Comparison is then made with the 1.61 manifold. Table 1 clearly

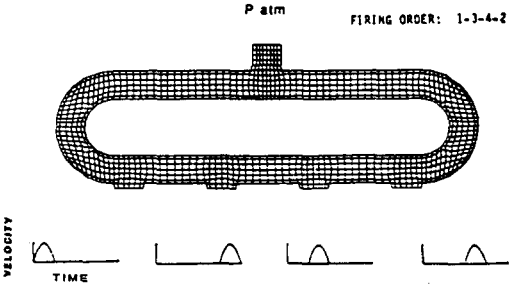

Figure 8. The concept loop-manifold.

shows the efficiency of the loop-manifold to be higher. This is reflected by the 3.6 % loss in the loop-manifold versus the 5.2 % loss in the 1.61 manifold. And there is no deterioration in the distribution of mass flow between each runner. The magnitude of the pressure fluctuations are smaller in figure 9 than those shown in figure 7. In addition, the pressure fluctuation between each runner are more similar for the loop manifold. This clearly demonstrates the use of "Flody" code in simulating different manifold flows not only to calculate their global losses but also to characterize their detailed dynamic behavior.

CONCLUSION

A computer simulation model of air flow inside an intake manifold for a 1.6 liter four cylinder engine has been developed using a fluid code. The code, called Flody, is based on the Conchas-Spray code developed at the Los Alamos

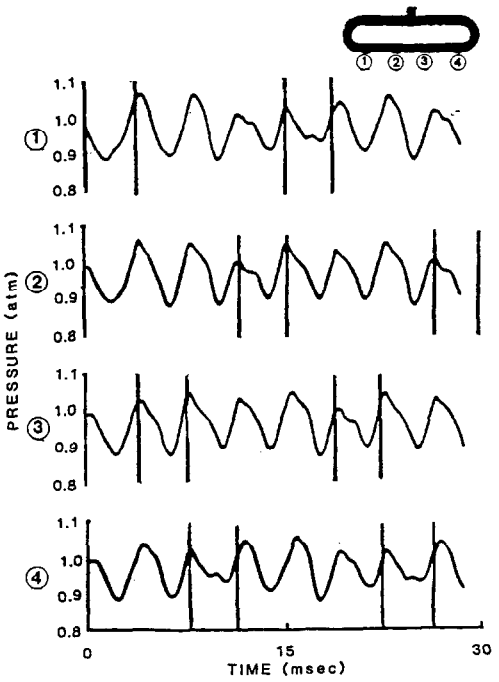

Figure 9. Pressure dynamics at outlets of loop-manifold.

National Laboratory. The flow is assumed to be two-dimensional, unsteady, compressible, and turbulent. A simplified subgrid scale (SGS) turbulence model is used. Hypothetical initial and boundary conditions are specified. Atmospheric pressure is assumed at the manifold inlet. The velocities at all the outlets are specified. The law of the wall boundary condition is used for the solid walls. Numerical results have been presented. The flow in a concept "loop manifold" is also simulated. Results presented show the later to have smaller manifold losses. An experimental effort is being carried out to investigate the validity of the numerical flow simulation.

REFERENCES

Amsden, A.A., and Hirt, C.W., "YAQUI: An Arbitrary Lagrangian-Eulerian Computer Program for Fluid Flow at All Speeds", Los Alamos Scientific Laboratory report LA-5100, March, 1973.

Amsden, A.A., Ruppel, H.M., and Hirt, C.W., "SALE: A Simplified ALE Computer Program for Fluid Flow at All Speeds", Los Alamos Scientific Laboratory report LA-8095, June, 1980.

Anderson, R.C., and Sandford II, M.T., "YOKIFER: A Two-Dimensional Hydrodynamics and Radiation Transport Program", Los Alamos Scientific Laboratory report LA-5704-MS, January, 1975.

Benson, R.S. "A Comprehensive Digital Computer Program to Simulate Compression Ignition Engine Including Intake and Exhaust Systems", SAE paper no. 710173, 1971.

Butler, T.D., Cloutman, L.D., Dukowicz, J.K., and Ramshaw, J.D., "CONCHAS: An Arbitrary Lagrangian-Eulerian Computer Code for Multicomponent Chemically Reactive Fluid Flow at All Speeds", Los Alamos Scientific Laboratory report LA-8129-MS, November, 1979.

Chapman, M. "Two Dimensional Numerical Simulation of Inlet Manifold Flow in a Four Cylinder Internal Combustion Engine", SAE paper no.790244, 1979.

Chapman, M., Novak, J.M., Stein, R.A. "Numerical Modeling of Inlet and Exhaust Flows in Multicylinder Internal Combustion Engines", ASME Winter Meeting Presentation, Phoenix, Arizona, Nov. 1982.

Cloutman, L.D., Dukowicz, J.K., Ramshaw, J.D., Amsden, A.A., " CONCHAS-SPRAY : A Computer Code for Reactive Flows with Fuel Sprays", Los Alamos Report No. LA-9294-MS, 1982.

Deardorff, J.W., Journal of Computational Physics, no. 7, p120, 1971.

Gosman, A.D., Khalil, E.E. and Whitelaw, J.H., "The Calculation of Two- Dimensional Turbulent Recirculating Flows", Proc. Symposium on Turbulent Shear Flows, Pennsylvania, 1977.

Hirt, C.W., "An Arbitrary Lagrangian- Eulerian Com puting Technique", Proc. Intern. Conf. Numerical Methods in Fluid Dynamics, 2nd, University of California, Berkeley, September 15-19, 1970, p350, Springer-Verlag, 1971.

Launder, B.E., Spalding, D..B., "Mathematical Models of Turbulence", Academic Press, 1972.

Low, S.C., Baruah, P.C., "A Generalized Computer Aided Design Package for I.C. Engine Manifold System", SAE paper no. 810498, 1981.

Patankar, S.V. Numerical Heat Transfer and Fluid Flow, McGraw Hill, 1980.

Pracht, W.E., and Brackbill, J.U., "BAAL: A Code for Calculating Three- Dimensional Fluid Flows at All Speeds with an Eulerian-Lagrangian Computing Mesh", Los Alamos Scientific Laboratory report LA-6342, August, 1976.

Schlichting, H., Boundary Layer Theory, McGraw Hill, 6th Edition, 1968.

Shimamoto, Y., et. al. "A Research on Inertia Charging Effect of Intake System in Multi-Cylinder Engines", JSME Bulletin p.502-510, vol.21, 1978.

Stein, L.R., Gentry, R.A., and Hirt, C.W., Comp. Meth. Appl. Mech. Eng. no. 11, p57, 1977.

Sullivan, D.A. "Historical Review of Real-Fluid Isentropic Flow Models", Transaction of ASME, pp.258-267, Vol. 103, June 1981.

Taylor, C.F., Livengood, J.C., Tsai, D.H. "Dynamics In The Inlet System of a Four-Stroke Single-Cylinder Engine", Transaction of ASME, p.1133-1145, vol.77, 1955.

Tunstall, J.N., "On the Derivation of Conservative Finite-Difference Expressions for the Navier-Stokes Equations", Union Carbide Corporation, Nuclear Division report K/CSD-5, Oak Ridge, Tenn., April, 1977.

Wu, H., Aquino, C.F., Chou, G.L. "A 1.6 Liter Engine and Intake Manifold Dynamic Model", ASME paper no. 83-WA/DSC-39, 1983.